PHYSICAL REVIEW A, VOLUME 64, 041601(R)

Ramsey-Bordé atom interferometer having two arms with different Zeeman sublevels

Shinya Yanagimachi, Kenji Mizobuchi, and Atsuo Morinaga
Department of Physics, Faculty of Science and Technology, Science University of Tokyo, 2641 Yamazaki, Noda-shi, Chiba 278-8510, Japan

(Received 15 February 2001; published 13 September 2001)

An atom interferometer, whose arms are in the different sublevels, was demonstrated using two σ^+- and two σ^--polarized, copropagating, laser beams in a magnetic field. Using the interferometer, Ramsey fringes with a width of 50 kHz were observed as a function of Zeeman shift frequency. The visibility of the interference fringes of 0.046 was obtained at an excitation power of almost $\pi/2$ pulse area.

DOI: 10.1103/PhysRevA.64.041601 PACS number(s): 03.75.Dg, 32.60.+i, 39.20.+q, 42.50.Vk

Over the past decade, atom interferometers have been developed as sensitive detectors for precise measurements and fundamental tests of quantum physics [1]. Ramsey-Bordé atom interferometers have been used successfully for such purposes [2–4]. The present authors have already developed symmetrical Ramsey-Bordé atom interferometers composed of three or four copropagating traveling laser beams and have achieved a visibility of 0.25 using a thermal calcium atomic beam [5–8].

These symmetrical atom interferometers work similar to white-light interferometers. Therefore, they are suitable for measuring a nondispersive phase shift that does not depend on the velocity of the atom, for example, the Aharonov-Casher (AC) effect [9]. In order to accurately measure the AC effect, two electrodes with opposite electric fields must be applied to two arms in the symmetrical interferometer. In our simple experiment, however, it was revealed that imperfect symmetry between the two electrodes introduces a residual dc Stark phase shift that washes out fringes as a result of dispersion.

In this study, we consider an atom interferometer comprised of two σ^+- and two σ^--polarized laser beams, where the atomic wave packets split into each of the two arms are in different Zeeman states of $m=1$ and $m=-1$. In principle, a single homogeneous electric field applied throughout the interferometer will generate the AC phase alone.

A few years ago, Hinderthür *et al.* developed an atom interferometer using a combination of polarized light fields of the same frequency and observed interference signals between coupled Zeeman-sublevel states [10]. Schmiedmayer *et al.* investigated the superposition of the eight independent interferometers comprised of atoms with the same magnetic moment in a weak magnetic field [11]. In the interferometer proposed here, atoms must be excited to the selected state at different frequencies for the σ^+- and σ^--polarized laser beams. This is the first attempt at the development of such an interferometer.

The conventional Ramsey-Bordé atom interferometer is based on a two-level atom having a ground state and a metastable excited state, and laser beams of frequency resonance to the transition between the states. For example, let us consider that the excited state has a quantum number of 1. As the upper level is split into $m=1$ and $m=-1$ states under the magnetic field B, two independent atom interferometers can be produced; one composed of the $m=1$ state and σ^+-polarized light, and the other composed of the $m=-1$ state and σ^--polarized light. The front half of the former interferometer and the rear half of the latter can be synthesized by driving the atoms with two σ^+-polarized light beams and two σ^--polarized light beams. The upper states of the two arms in the synthesized interferometer are different; $m=1$ and $m=-1$. Realizing the synthesis of two interferometers will be significantly valuable for increasing the applicability of atom interferometers.

In this Rapid Communication, we present the principle of the synthesized atom interferometer and demonstrate the interference fringes and Ramsey resonance as a function of magnetic-field strength.

Figure 1 shows the configuration of the interferometer. We consider the Ca atom as a two-level state atom. The ground state is the $^1S_0$ state and the excited state is the $^3P_1$ state with a lifetime of 0.57 ms [12]. The atomic beam in the ground state moves in the x direction and interacts with the four laser beams, which propagate along the z direction, through a homogeneous magnetic field also applied in the z direction. The frequency of the laser beams is resonant to the transition $^1S_0 \rightarrow {}^3P_1$. The first and the second laser beams

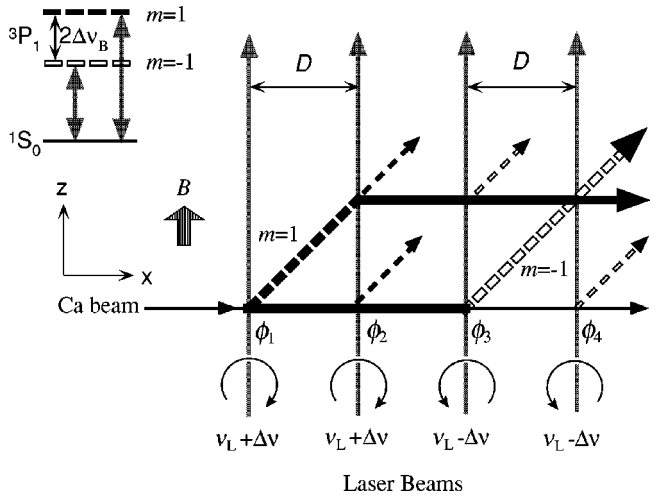

FIG. 1. Scheme of the synthesized atom interferometer in magnetic field B, and level diagram of calcium. Solid line, ground state; broken black line, excited $m=1$ state; broken white line, excited $m=-1$ state; ϕ_i, phase of ith laser beam (gray line); frequency and polarization of laser beams are shown in the figure.

are circularly σ^+-polarized and shifted in frequency $+\Delta\nu$ from the carrier frequency of the laser, ν_L. In contrast, the third and the fourth beams are circularly σ^--polarized and shifted in frequency $-\Delta\nu$ from ν_L. The frequency shift $\Delta\nu$ is close to the Zeeman frequency shift $\Delta\nu_B=\mu_B B/h$, ϕ_i is the phase of the ith laser beam at $z=0$, and the beam spacing D between the first and second laser beams is equal to that between the third and fourth laser beams.

In the first interaction of the atoms and the laser beam, part of the atomic beam is excited to the $^3P_1$, $m=1$ state with recoil velocity v_r in the z direction (upper arm). In the second interaction, with the σ^+ laser beam, the atom in the upper arm emits light due to the stimulation and reverts to its original direction of motion. In the third interaction, with the σ^- laser beam, atoms in the lower arm absorb photons and are excited to the $^3P_1$, $m=-1$ state and deflected. In the final interaction, with the σ^- laser beam, atoms in the upper arm are excited again to the $^3P_1$, $m=-1$ state and the two arms in the $m=-1$ state (or ground state) overlap.

The phase difference between atoms in the $m=-1$ state, after having passed through the upper or lower arm, can be calculated based on the phase shift arising from the interaction of the atom with light $\Delta\psi_L$ and the phase shift due to the free evolution of atoms between interactions $\Delta\psi_A$. The former phase shift is given by

$$\Delta\psi_L=(\pi-\phi_1+\phi_2-\phi_3-\phi_4)+4\pi\Delta\nu\left(\frac{D}{v_x}\right)-4\pi\Delta\nu\left(\frac{v_z+v_r}{c}\right)\frac{D}{v_x}, \quad (1)$$

where v_x and v_z are the initial velocities of atoms in the x and z directions. The first term represents the phase difference of the four laser beams, and the second and the third terms represent the frequency difference between the σ^+ and σ^- beams. The third term can be ignored because it is smaller than the second term by a factor of $(v_z+v_r)/c$, or $\sim 10^{-8}$.

Under the perturbation of the magnetic field, the latter phase shift occurs due to the dynamical Zeeman effect, according to

$$\Delta\psi_A=\frac{-4\pi\Delta\nu_B D}{v_x}. \quad (2)$$

The total phase shift $\Delta\psi$ is then given by

$$\Delta\psi=(\pi-\phi_1+\phi_2-\phi_3-\phi_4)+2\pi(\Delta\nu-\Delta\nu_B)\left(\frac{2D}{v_x}\right). \quad (3)$$

Therefore, the phase shift does not depend on the carrier frequency of the laser, as is the case in a conventional symmetrical atom interferometer [5]. When $\Delta\nu$ exactly equals the Zeeman frequency shift, the total phase shift is independent of the atomic velocity. It should be noted that Ramsey fringes of period $v_x/2D$ appear as a function of the frequency difference between $\Delta\nu$ and $\Delta\nu_B$.

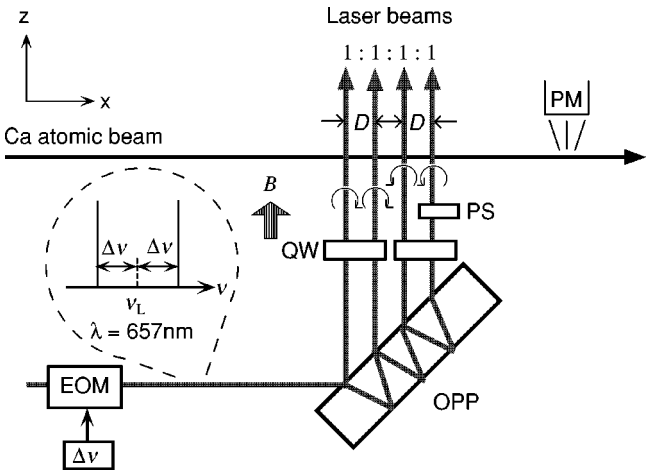

FIG. 2. Experimental setup for the synthesized atom interferometer. PM, photomultiplier; PS, phase shifter; QW, quarter-wave plate; OPP, optical parallel plate; EOM, electro-optic modulator.

The population probability bb^* of atoms in the excited state after four interactions with light is given by

$$bb^*=2\alpha^2\beta^2+2\alpha^2\beta^6+2\alpha^6\beta^2+2\alpha^4\beta^4\cos\Delta\psi, \quad (4)$$

where α denotes the amplitudes of the interaction with light when the state of the atom has not changed, and β denotes that when the state has changed. Other terms with a phase of v_zT are omitted because those terms vanish upon the integration of v_z, assuming that the mean value of v_zT is large compared to the optical wavelength. The last term represents the interference fringes and the other terms represent the background. The visibility of the interference fringes was calculated using Eq. (4), taking into account the specific features of the Ca atomic beam device; the divergent thermal atomic beam, the transit time broadening, and the Maxwellian velocity distribution [7,8]. The visibility was calculated to be 0.088 at an excitation power of the $\pi/2$ pulse area for atoms with the most probable velocity.

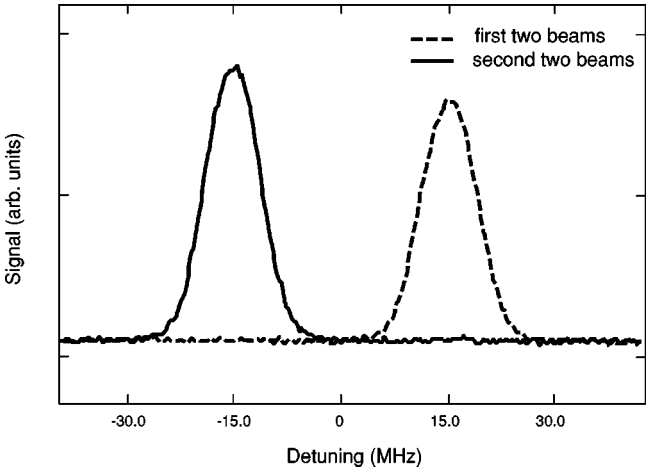

FIG. 3. Fluorescence signal from the excited state for excitations of the first two beams (dashed line), and second two beams (solid line), as a function of detuning from the transition frequency between $^1S_0$ and $^3P_1$ of the $m=0$ state.

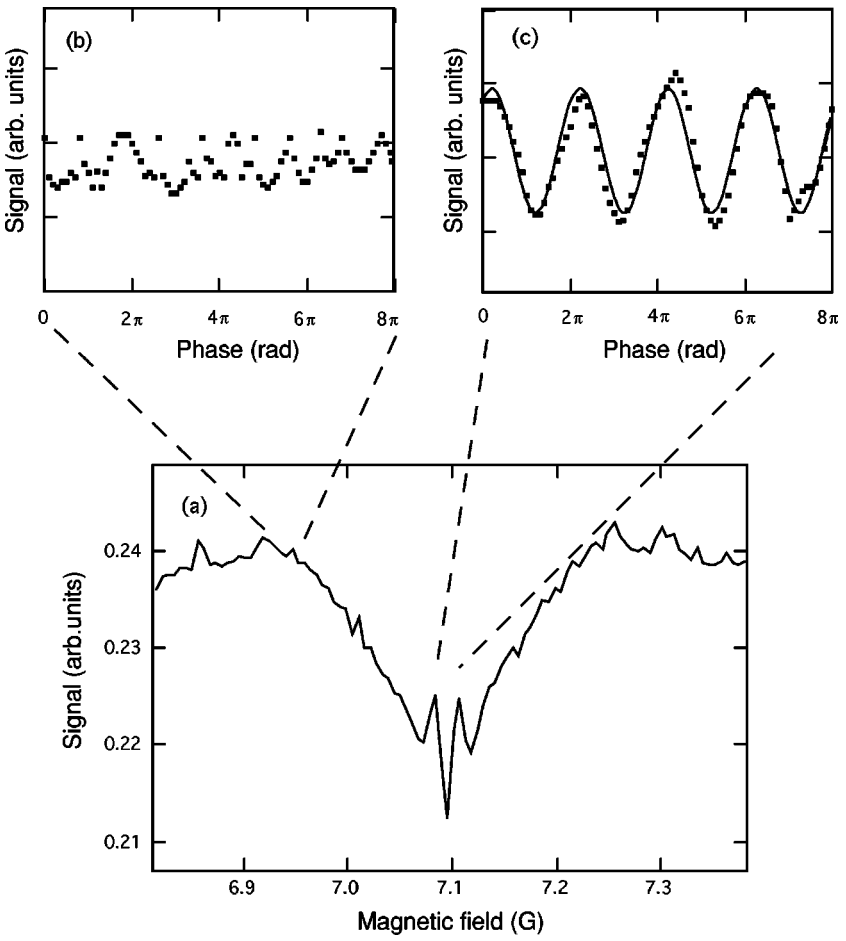

FIG. 4. Experimental results. (a) Ramsey fringe as a function of magnetic-field strength. Signals are detected at an integration time of 0.1 s every 6 mG. (b) Fluorescence signal under a magnetic field of 6.93 G as a function of phase. (c) Fluorescence signal together with a sinusoidal curve (solid line) under a magnetic field of 7.09 G as a function of phase.

Our experimental setup is shown in Fig. 2. A thermal calcium atomic beam was generated from the oven at a temperature of 700 °C, which corresponds to the most probable velocity of 780 m/s. The atomic beam was collimated so that a residual Doppler full-width at half maximum was about 8 MHz. An output beam with a wavelength of 657 nm from a high-resolution diode laser spectrometer was used to excite the Ca atoms to the $^3P_1$ state from the ground state $^1S_0$. The frequency of the diode laser was stabilized to the high stable reference cavity by the frequency-modulated sideband technique, and the oscillation linewidth was estimated to be less than 100 kHz. The laser power was amplified to approximately 20 mW using an injection-locked diode laser. The output beam was introduced into a resonant-type electro-optic modulator driven at a 14.9 MHz with a modulation index of 2.1. One sideband frequency of $\nu_L + 14.9$ MHz was used as the σ^+-polarized beam and the other of $\nu_L - 14.9$ MHz was used as the σ^--polarized beam. The fractional power of one sideband was 30% of the incident beam. The magnetic field was produced by a Helmholtz coil and the fluctuation of the magnetic field in the region of the interferometer was about 0.1%.

In order to generate the four parallel laser beams copropagating in the same direction with equal beam spacing and equal power, a special beam splitter was developed. The optical parallel plate was 60 mm long and 11 mm thick. The surface roughness was one tenth of wavelength used, and the parallelism was within 2 s [7]. The front surface was divided into four sections, each of which had a dielectric coating with a different reflectivity for the *S*-polarization wave at an incident angle of 45°. The rear surface had a perfect reflective coating. Using this beam splitter, four parallel laser beams with an intensity ratio of 1.0:0.8:0.9:0.9 were produced with a beam spacing of 8.3 mm.

Quarter-wave plates were inserted after the beam splitter in order to give the first and the second laser beams σ^+

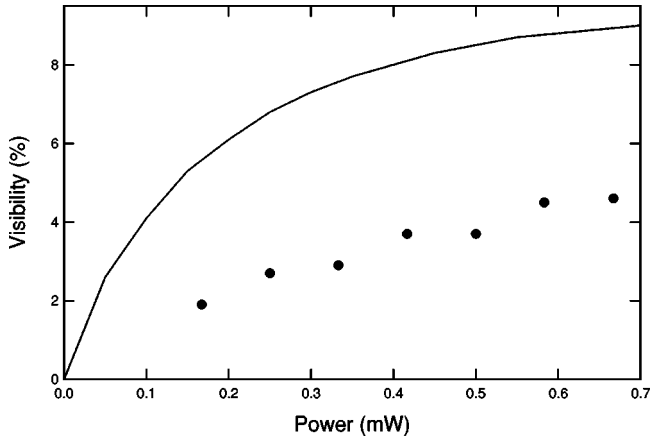

FIG. 5. Visibility versus the excitation laser power, together with the calculated curve.

circular polarization and the third and fourth laser beams σ^- polarization. A phase plate was inserted in the path of the fourth beam before interaction with the atomic beam. The population probability of the upper state was observed by monitoring the fluorescence from the $^3P_1$ state approximately 300 mm downstream from the excitation region. By changing the angle of the phase plate, interference fringes appeared in the fluorescence signal.

The fluorescence spectrum of atoms excited by only the first two laser beams (σ^+-polarized beam) is shown in Fig. 3. The spectrum shows that the $m=1$ state was excited over 100 times greater than the state of $m=-1$. Thus, the extinction ratio of σ^+ (σ^-) to σ^- (σ^+) was less than 0.01 in the best alignment. Therefore, the interference signal of atom interferometers comprising only the $m=1$ state or $m=-1$ state can be effectively attenuated.

The laser beam diameter was 3 mm in the interaction zone, and the optimum power for each laser beam was 0.6 mW, which corresponds to the $\pi/2$ pulse area for atoms with the most probable velocity [13]. The apparatus was adjusted in order to obtain as much visibility as possible using the conventional symmetrical interferometer with the four equally spaced laser beams [14]. At the excitation power of 0.65 mW, we obtained a visibility of 0.14, which is lower than the calculated visibility of 0.25 for the conventional symmetrical atom interferometer.

Figure 4(a) shows the fluorescence signal excited by two σ^+ polarization beams and two σ^- polarization beams when the magnetic field was near a Zeeman frequency shift of 14.9 MHz. At the Zeeman frequency shift of 14.9 MHz, a saturation dip appears with a depth of about 15% and a full width at half maximum of about 400 kHz, which corresponds to the transit width. Near the center dip, Ramsey fringes with a period of 50 kHz can be seen. This period is almost equal to $v_x/(2D)$. Figures 4(b) and 4(c) show the fluorescence signals as a function of phase when the phase plate was rotated. (b) was obtained in a magnetic field of 6.93 G, while (c) was obtained at 7.09 G. Clear interference fringes with a visibility of 0.046 at a sideband power of 0.65 mW can be seen in (c), whereas interference fringes are not seen in (b). The reason for this is that the σ^+ polarization beam and σ^- polarization beam interact with the atoms with the same velocity v_z in case of (c), whereas in (b), they interact with atoms having different velocities.

The dependence of visibility on the power of one sideband is shown in Fig. 5, together with the visibility calculated from Eq. (4). The visibility becomes almost constant above 0.6 mW, which corresponds to the $\pi/2$ pulse area for atoms with the most probable velocity. Consequently, the maximum visibility is estimated to be 0.046. The behavior observed in the experimental results is similar to the calculated behavior, but the value is almost half the calculated magnitude. The ratio of the experimental value to the calculated value is almost the same as that for the symmmetrical atom interferometer with four equally spaced laser beams. The visibility obtained might be appropriate to the experimental conditions, and there is a still room for improvement of the experiment.

In conclusion, we have successfully developed an atom interferometer with $m=1$ and $m=-1$ states in its arm by the synthesis of two atom interferometers, one of which comprises the $m=1$ state and σ^+-polarized laser beam, and the other comprises the $m=-1$ state and a σ^--polarized laser beam. The interference fringes occur when the frequency shift of both the σ^+- and σ^--polarized laser beams is resonant to the Zeeman frequency shift. Ramsey fringes were observed as a function of the magnetic-field strength. This atom interferometer will be useful for nondispersive phase measurement of the Aharonov-Casher effect.

The authors acknowledge Dr. J. Helmcke and Dr. F. Riehle for their valuable discussions and kind collaborations. We also thank to Dr. T. Kurosu for an introduction to the diode-laser system, and M. Kajiro for his assistance with experimental equipment. This research was partly supported by a Grant-in-Aid for Scientific Research on Priority Area (B), Research of the Ministry of Education, Science, Sports and Culture (Japan).

[1] See, e.g., *Atom Interferometry*, edited by P.R. Berman (Academic, San Diego, 1997).
[2] F. Riehle, Th. Kisters, A. Witte, J. Helmcke, and Ch.J. Bordé, Phys. Rev. Lett. **67**, 177 (1991).
[3] M. Kasevich and S. Chu, Phys. Rev. Lett. **67**, 181 (1991).
[4] K. Zeiske, G. Zinner, F. Riehle, and J. Helmcke, Appl. Phys. B: Lasers Opt. **60**, 205 (1995).
[5] A. Morinaga and Y. Ohuchi, Phys. Rev. A **51**, R1746 (1995).
[6] A. Morinaga, M. Nakamura, T. Kurosu, and N. Ito, Phys. Rev. A **54**, R21 (1996).
[7] S. Yanagimachi, Y. Omi, and A. Morinaga, Phys. Rev. A **57**, 3830 (1998).
[8] Y. Omi and A. Morinaga, Appl. Phys. B: Lasers Opt. **67**, 621 (1998).
[9] Y. Aharonov and A. Casher, Phys. Rev. Lett. **53**, 319 (1984).
[10] H. Hinderthür, A. Pautz, F. Ruschewitz, K. Sengstock, and W. Ertmer, Phys. Rev. A **57**, 4730 (1998).
[11] J. Schmiedmayer, C.R. Ekstrom, M.S. Chapman, T.D. Hammond, and D.E. Pritchard, J. Phys. II **4**, 2029 (1994).
[12] R. Druzdowski, J. Kwela, and M. Walkiewicz, Z. Phys. D: At., Mol. Clusters **27**, 321 (1993).
[13] F. Riehle, A. Morinaga, J. Ishikawa, T. Kurosu, and N. Ito, Jpn. J. Appl. Phys., Part 2 **31**, L1542 (1992).
[14] T. Trebst, PTB Report No. PTB-Opt-60, 1999 (unpublished).